Electronic Supplementary Material (ESI) for Journal of Materials Chemistry A.

Plasmonically driven photocatalytic hydrogen evolution activity of Pt-functionalized Au@CeO_2 core-shell under visible light

Dung Van Dao,[†,‡] Thuy T.D. Nguyen,[‡] Thanh Duc Le,[‡] Seung-Hyeon Kim,[§] Jin-Kyu Yang,[§] In-Hwan Lee,[*,] and Yeon-Tae Yu,[*,‡]

[†] Institute of Research and Development, Duy Tan University, Danang 550000, Vietnam

[‡] Division of Advanced Materials Engineering and Research Center for Advanced Materials Development, Chonbuk National University, Jeonju 54896, South Korea

[§] Department of Optical Engineering, Kongju National University, Cheonan 31080, Republic of Korea

Department of Materials Science and Engineering, Korea University, Seoul 02841, South Korea

Experimental section

Chemicals

All chemicals were of analytical grade and used without any further purification. Chloroauric acid (99.99%) and cerium (III) nitrate hexahydrate (99.99%) were purchased from Sigma Aldrich. 2-propanol (99.5%), methanol (99.8%), sulfuric acid (98.08%), nitric acid (63.01%), hydrochloric acid (37%), and trisodium citrate hydrate (98%) were supplied by Showa Chemicals. Hydrogen hexachloroplatinate (IV) hydrate (99.9%) was provided by Kojima Chemicals. Sodium carbonate anhydrous (99.00%) was obtained by Duksan Pure Chemicals.

Hydrothermal synthesis of Au@CeO_2-Pt core–shell photocatalyst

The 1.0 mM chloroauric acid (250 mL) was first heated to the boiling point, followed by the addition of a 34 mM trisodium citrate solution (25 mL) as the reducing argent. The color of the resulting suspension became deep violet after 10 s; after 1 min, the blue color abruptly turned into brilliant red, indicating the formation of spherical Au NPs. The solution was maintained at 97°C for 15 min under stirring. Then, it was naturally cooled down to room temperature and the suspension color changed into pink. Next, 10 mL of the as-prepared Au solution was added into distilled water and ultrasonicated for 5 min, followed by the injection of a 5 mM Na_2CO_3 solution (45 mL) under stirring for 10 min at room temperature and the successive addition of a 5 mM $Ce(NO_3)_3$ solution (10 mL) via slow dropping under further stirring for 10 min. The reaction was performed at 90°C for 12 h under stirring and, then, the solution was cooled to room temperature. The color of the as-obtained Au@CeO_2 suspension turned into intense purple, indicating the successful formation of the CeO_2 shell on the Au core.

For the Au@CeO_2-Pt synthesis, 30 mL of this Au@CeO_2 colloid was ultrasonicated for 10 min, followed by the addition of a 0.1 M Pt^{4+} solution (1.0 mL) under stirring for 15 min at room temperature and the

successive injection of a 34 mM trisodium citrate solution (15 mL). The resulting solution was heated at 90 °C for 4 h and, then, cooled to room temperature naturally. Its color turned into brown. After that, the Au@CeO_2-Pt precipitates were separated by centrifugation at 18,000 rpm for 30 min. Finally, the collected powders were washed with distilled water and absolute ethanol several times and, then, calcined at 500°C in air for 2 h to obtain the desired Au@CeO_2-Pt core–shell photocatalyst. In addition, a pure CeO_2 photocatalyst was also prepared using the same above-described method without adding Au colloid and Pt salt.

Characterization

The morphology of the prepared photocatalysts was investigated via high-resolution transmission electron microscopy (HRTEM) with a JEM-2010 microscope (JEOL) operated at 200 kV. The crystal structure of Au@CeO_2-Pt was analyzed by using an X-ray diffractometry (XRD) system (D/Max 2005, Rigaku) and Cu Kα radiation (λ = 1.54178 Å). The changes in the SPR peaks were observed via ultraviolet–visible light (UV–vis) transmission spectroscopy with an Agilent/HP 8453 spectrophotometer at room temperature. X-ray photoelectron spectroscopy (XPS) was performed with a Multilab 2000 instrument (Thermo Fisher Scientific) and monochromated Al Kα radiation (hv = 1,486.6 eV) to investigate the surface chemical states of the elements present in the synthesized photocatalysts; the calibration was based on the binding energies of the adventitious C 1s peak at around 285 eV. The surface areas of the samples were estimated via the nitrogen gas adsorption method so to generate high-quality data by performing the Barrett–Emmett–Teller (BET) technique with a Micromeritics Tristar 3000 analyzer. The spatial distribution of the electric field intensity surrounding the Au@CeO_2-Pt NPs was calculated through three-dimensional (3D) finite-difference time-domain (FDTD) simulations; the grid size was set at 1 nm (0.001 nm^3 in volume), the incident light wavelength was 550 nm, and the photocatalyst was surrounded by water (n = 1.33). The microstructure of the sample and electrode for photoelectrocatalytic tests was

further examined with a scanning electron microscopy (SEM) instrument (Hitachi, S-4800). The inductively coupled plasma (ICP) spectrometry (ICPS-7500, Shimadzu) was used for measuring the Pt losing after stability tests. The ICP samples were treated with aqua regia at 100 °C for 10 h and were carefully filtered to remove solid components.

Electrochemical measurements

The Au@CeO_2-Pt photocatalyst was dispersed in a mixture of distilled water, 2-propanol, and Nafion solution. The resulting slurry was ultrasonicated at room temperature for 1 h to obtain a uniform solution; then, it was sprayed on a carbon cloth substrate to obtain an Au@CeO_2-Pt/C electrocatalyst. Finally, the as-obtained electrode was dried at 60 °C for 12 h before use. Its electrochemical properties were investigated by using a three-electrode setup (Gamry Instruments Reference 3000, Potentiostat/Galvanostat/ZRA) with and without visible light irradiation from a 300 W xenon lamp (Asahi, Max 303). Electrochemical impedance spectroscopy (EIS) was performed in a 0.25 M H_2SO_4 + 1 M CH_3OH electrolyte at 25 °C from 100 kHz to 0.05 Hz. The methanol oxidation reaction (MOR) was conducted in a 0.25 M H_2SO_4 + 1 M CH_3OH electrolyte at 25 °C and a sweep rate of 50 mV s^{-1}. During the tests, the electrolyte was purged with pure N_2 to prevent the attack from oxygen.

Photocatalytic hydrogen evolution

The photocatalytic HER of pure CeO_2, Au@CeO_2 and Au@CeO_2-Pt was performed via the water displacement technique. First, each photocatalyst (50 mg) was dispersed in a 25% CH_3OH solution (50 mL) as the sacrificial reagent. Prior to visible light irradiation ($\lambda > 420$ nm) with a, the solutions were stirred for 30 min in dark condition to ensure the adsorption/desorption equilibrium of the reactants on the surface of the dispersed NPs; concurrently, air was totally removed from the reaction solution by purging with pure nitrogen. The reaction time for each cycle was fixed at 2 h. After the completion of each run,

the photocatalyst was isolated and dried at 100 °C for 2 h before reuse. Then, the so-produced hydrogen gas was analyzed with a gas chromatograph (Shimadzu, GC-2010). The photocatalytic hydrogen production activity for the same samples (CeO_2, Au@CeO_2, and Pt-functionalized Au@CeO_2) is tested at around 550 nm using 50 W xenon lamp to confirm the photocatalytic activity of CeO_2 and Au parts using 50 W xenon lamp. The apparent quantum yield (AQY) efficiencies for hydrogen evolution reaction at around 550 nm for the prepared photocatalysts are calculated by using the following equation:

$$AQY\ efficiency\ [\%] = \frac{Numbers\ of\ evoluted\ hydrogen\ molecules\ x\ 2}{Numbers\ of\ incident\ photons}\ x\ 100$$

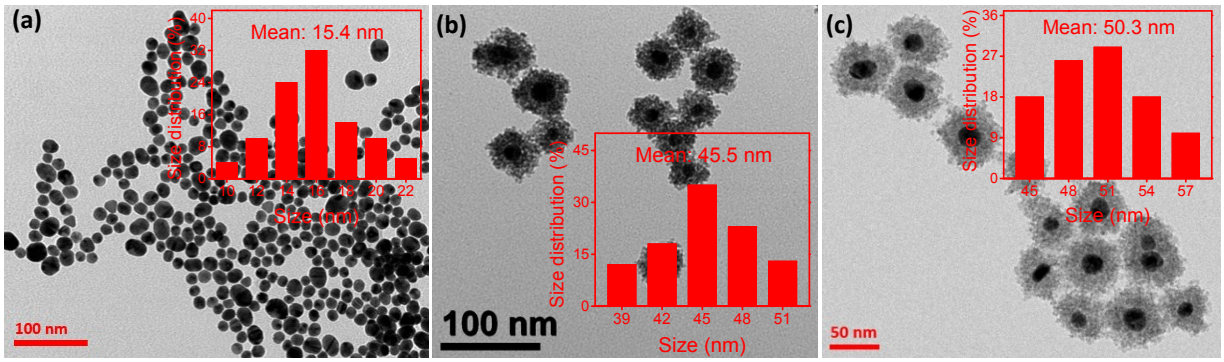

Fig. S1 (a) TEM analysis of Au, Au@CeO_2, and Au@CeO_2-Pt materials.

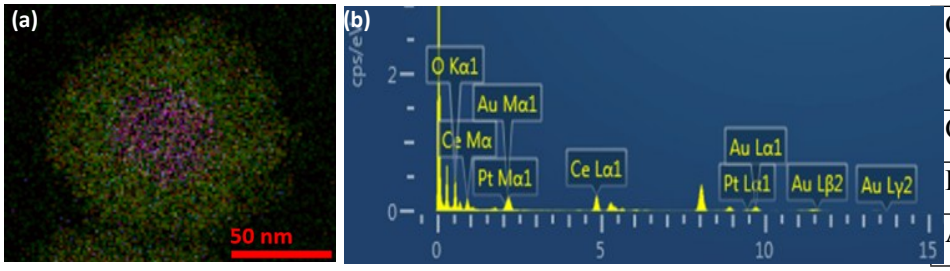

Component	Wt.%
O	26
Ce	45
Pt	4
Au	25

Fig. S2 (a) High-resolution TEM overlay mapping and (b) EDS spectrum of Au@CeO_2-Pt photocatalyst.

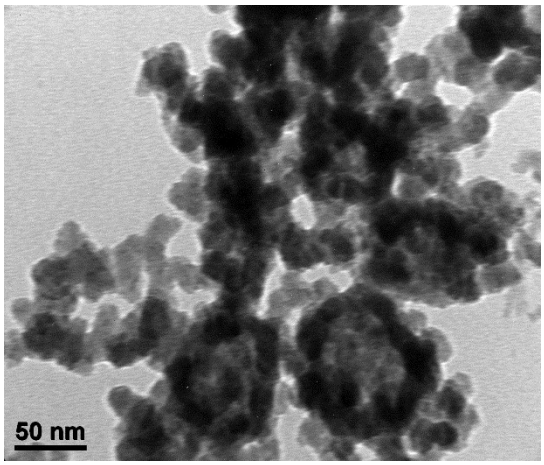

Fig. S3 TEM image of pure CeO_2.

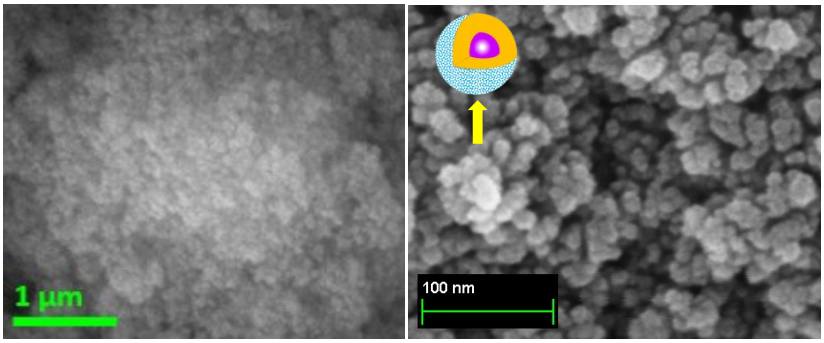

Fig. S4 SEM analysis of as-calcined Au@CeO_2-Pt photocatalysts.

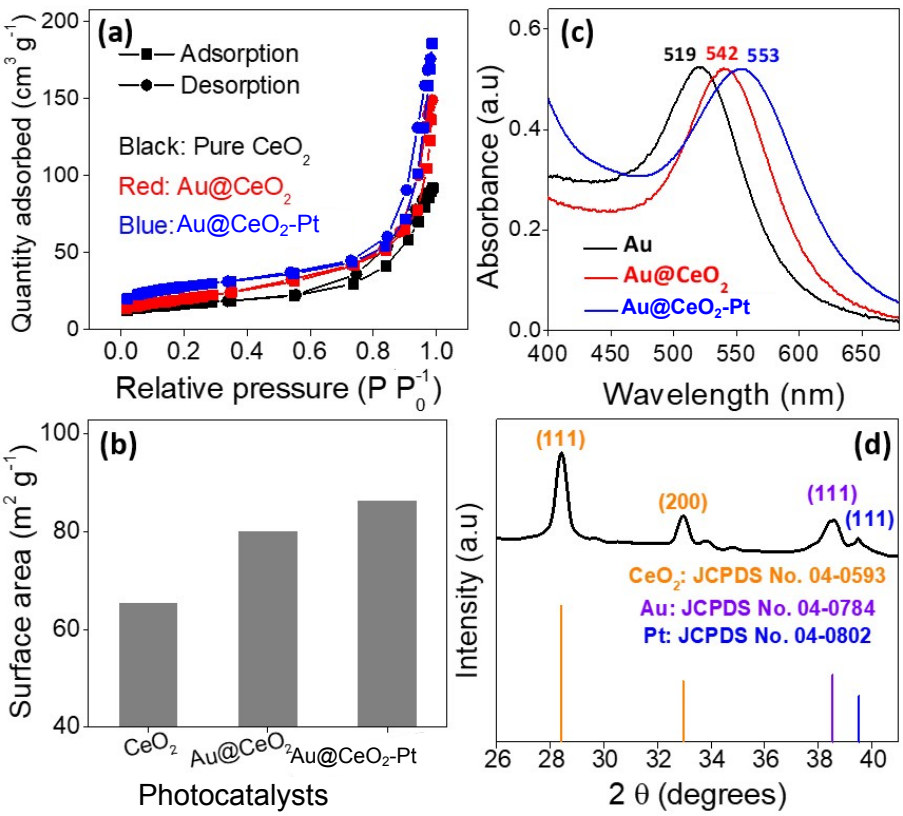

Fig. S5. (a) Nitrogen adsorption/desorption isotherms of pure CeO_2, Au@CeO_2, and Au@CeO2-Pt photocatalysts and (b) corresponding BET surface areas. (c) Ultraviolet–visible light absorption spectra of Au, Au@CeO2, and Au@CeO2-Pt suspensions. (d) X-ray diffraction pattern of Au@CeO2-Pt; the CeO2, Au, and Pt peaks are marked in yellow, purple, and blue.

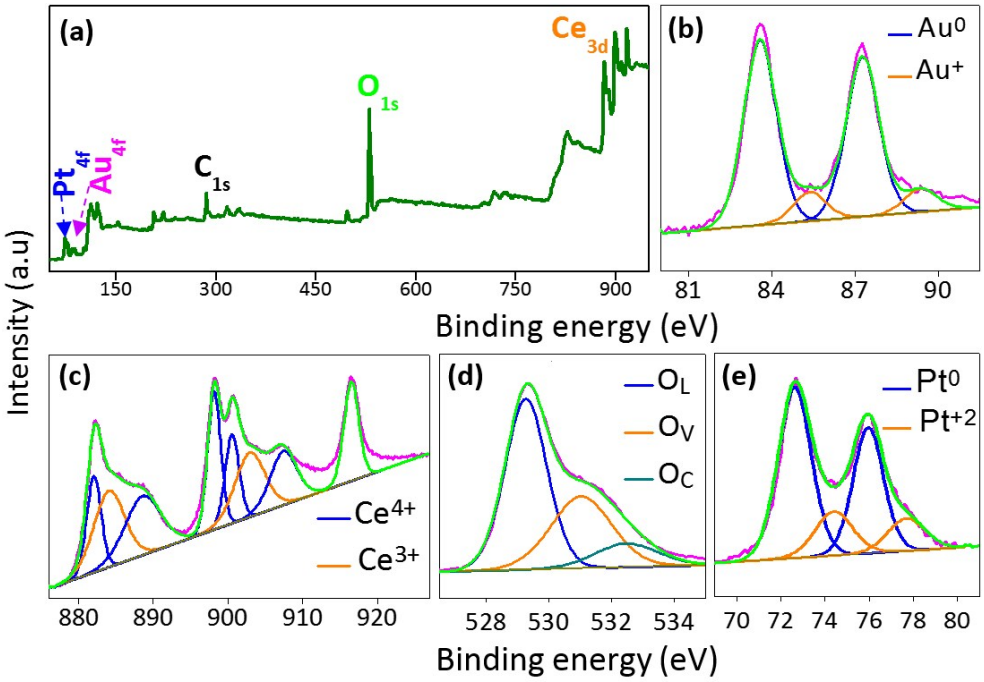

Figure S6. X-ray photoelectron spectra of Au@CeO_2-Pt: (a) full survey spectrum and (b) Au 4f, (c) Ce 3d, (d) O 1s, and (e) Pt 4f spectra.

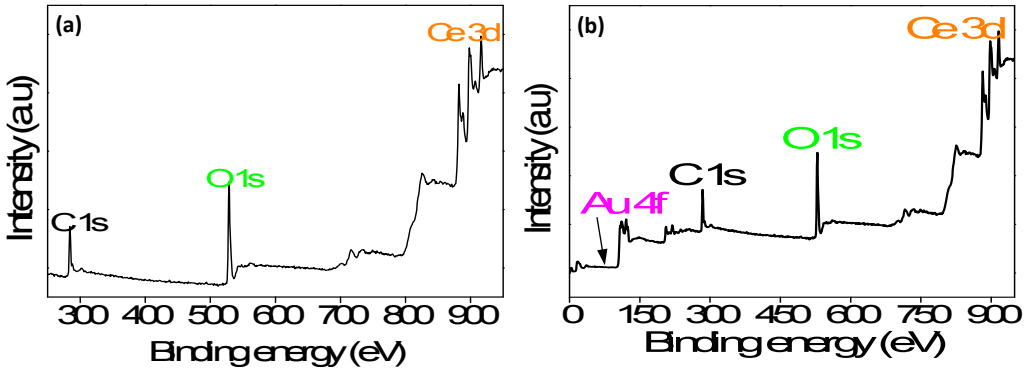

Fig. S7 Full XPS spectrum of (a) CeO_2 and (b) Au@CeO_2 photocatalysts.

Table S1. Summary of the XPS analysis of Au 4f, Ce 3d, and O 1s in pure CeO_2, Au@CeO_2, and Au@CeO_2-Pt photocatalysts.

Catalysts	$Au^+/(Au^+ + Au)$		$Ce^{3+}/(Ce^{3+} + Ce^{4+})$		Oxygen		
	Energy (eV)	Percentage (%)	Energy (eV)	Percentage (%)	Species	Energy (eV)	Percentage (%)
CeO_2	-	-	884.40 902.80	18.56	O_L	529.11	47.64
					O_V	530.66	15.24
					O_C	532.38	37.12
Au@CeO_2	84.89 88.97	13.0	885.52 903.45	31.69	O_L	529.23	52.83
					O_V	530.94	29.59
					O_C	532.00	17.58
Au@CeO_2-Pt	85.41 89.39	12.5	884.16 903.04	30.22	O_L	529.20	53.20
					O_V	530.98	28.46
					O_C	532.32	18.34

O_L: Lattice oxygen; O_V: Oxygen vacancy; O_C: chemisorbed oxygen.

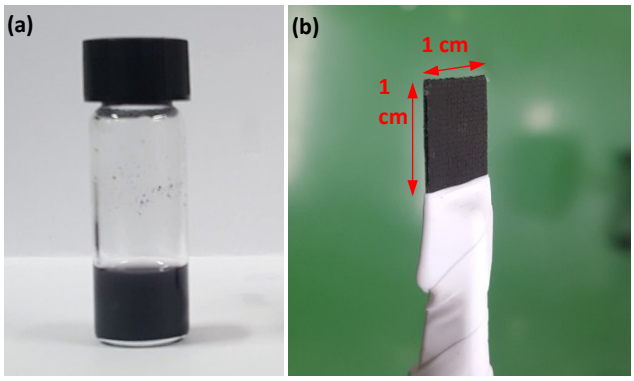

Fig. S8 (a) Au@CeO_2-Pt slurry and (b) corresponding electrocatalyst for electrochemical property tests.

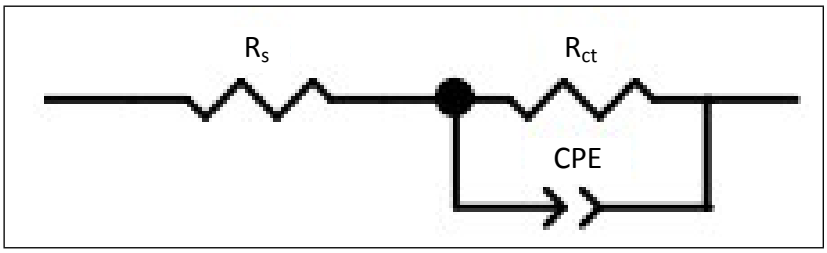

Fig. S9 An electrical equivalent circuit used to fit the Nyquist plots: R_s indicates the solution resistance, R_{ct} presents the charge transfer resistance, and CPE is a constant phase element.

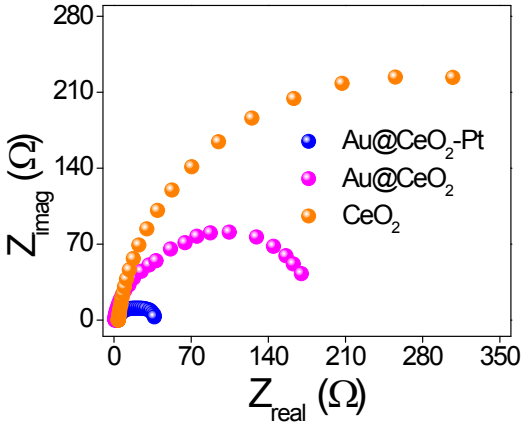

Fig. S10 An electrical equivalent circuit used to fit the Nyquist plots: R_s indicates the solution resistance, R_{ct} presents the charge transfer resistance, and CPE is a constant phase element.

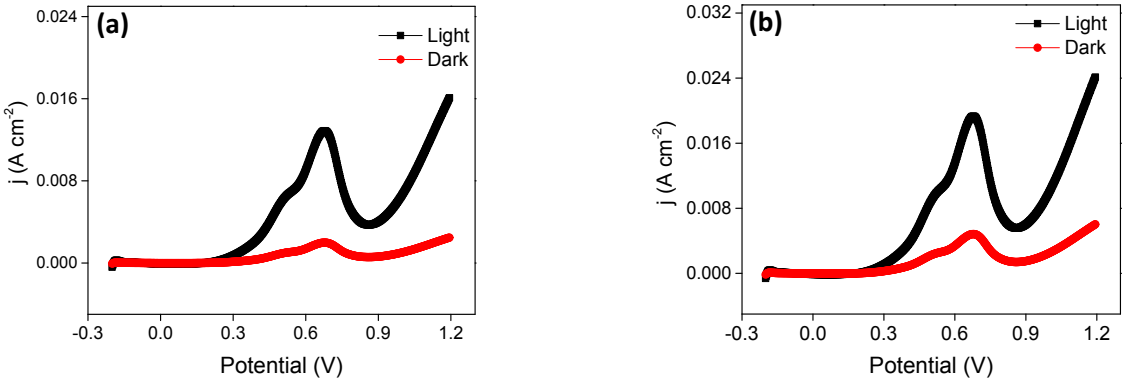

Fig. S11 MOR activity of (a) CeO_2 and (b) Au@CeO_2 photoelectrocatalysts under dark and light.

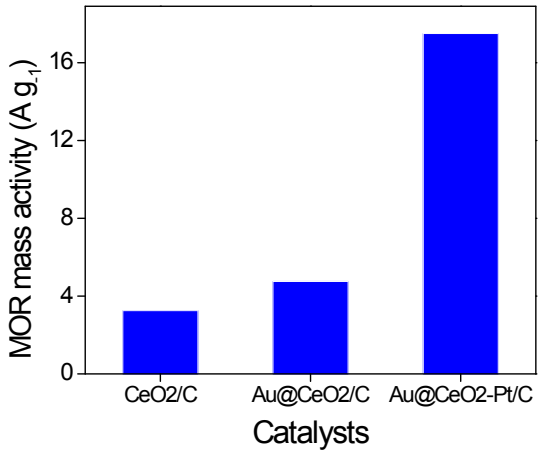

Fig. S12 Comparison of MOR mass activity between CeO_2/C, Au@CeO_2/C and Au@CeO_2-Pt/C electrodes.

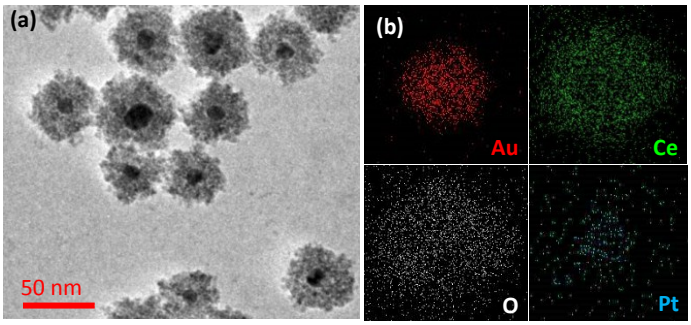

Fig. S13 High-resolution TEM analysis of as-used Au@CeO_2-Pt after photocatalytic hydrogen evolution stability test: (a) structural image preservation of core-shell photocatalysts and (b) corresponding mapping confirmation.

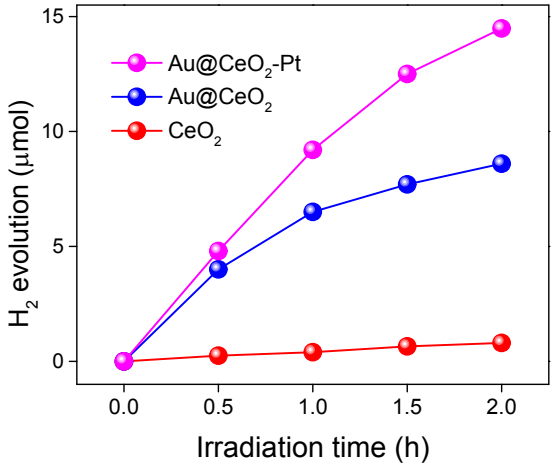

Fig. S14 Time-dependent hydrogen production by the pure CeO_2, $Au@CeO_2$, and Pt-functionalized $Au@CeO_2$ photocatalysts at 550 nm.

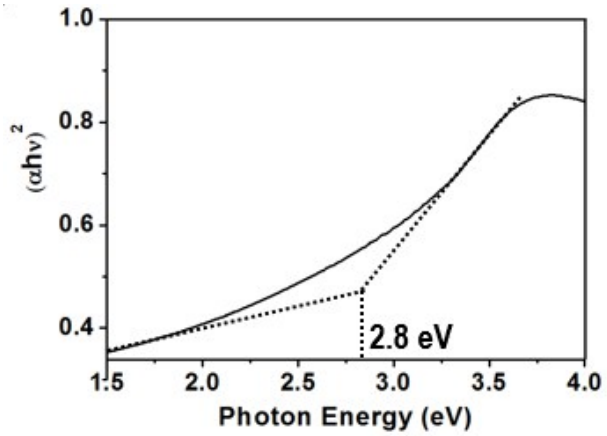

Fig. S15 The plot of $(\alpha h\nu)^2$ vs. photon energy (eV) of pure CeO_2.

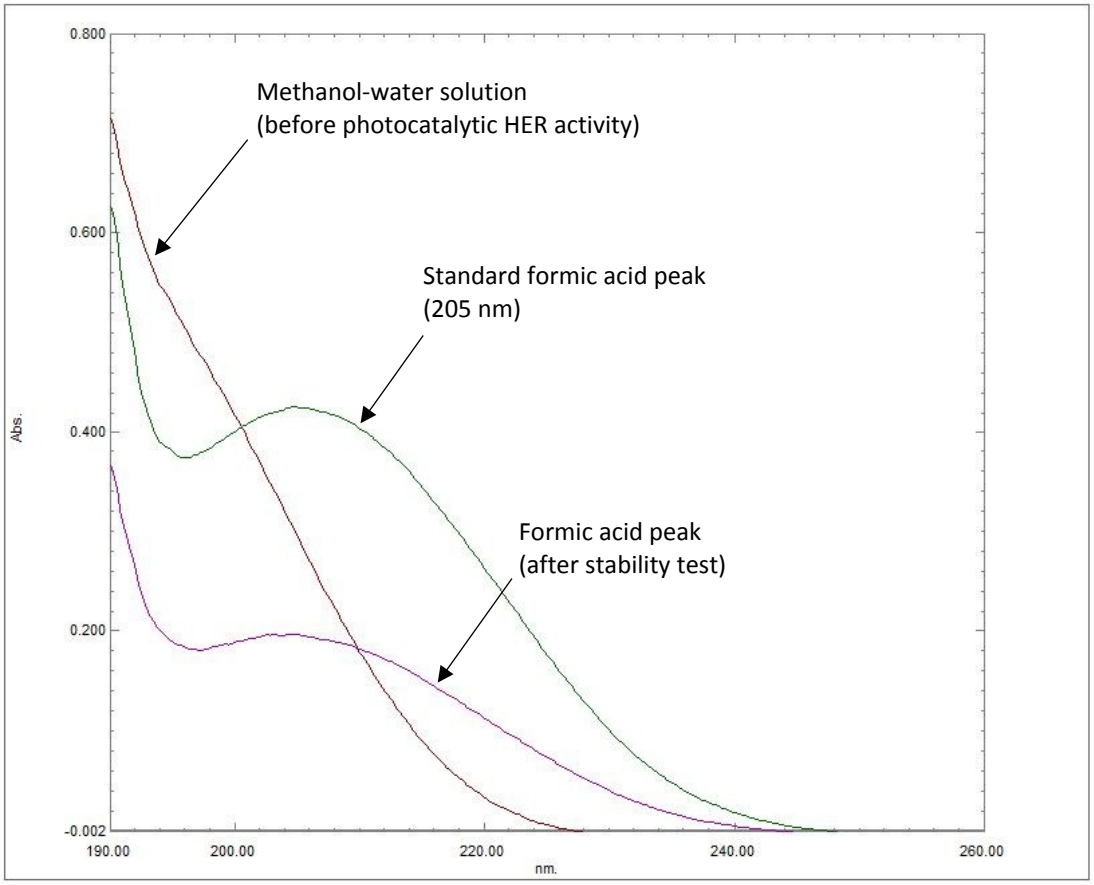

Fig. S16 UV spectra of solutions before and after photocatalytic hydrogen evolution stability tests using Pt-functionalized Au@CeO_2 core-shell catalysts.

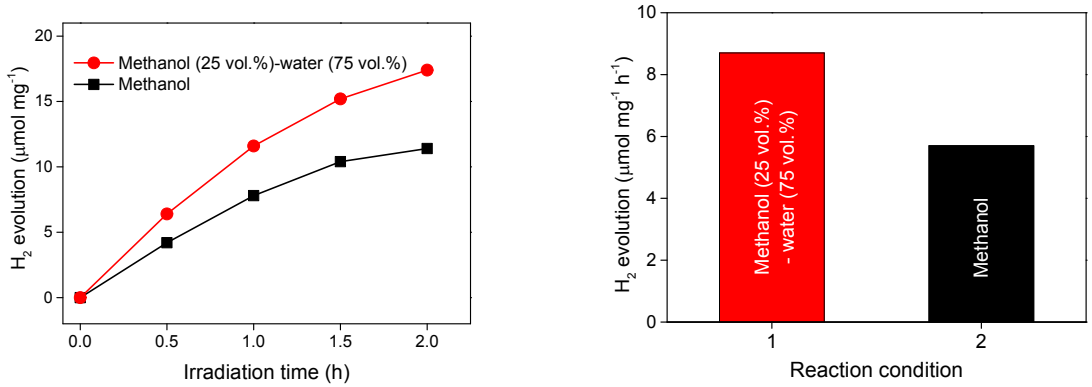

Fig. S17 Comparison of hydrogen evolution performance in methanol-water and methanol solutions for Pt-functionalized Au@CeO_2 core-shell photocatalyst.